Article

Optimal Waveform of the Partial-Respond Signal Based on Minimum Out-of-Band Radiation Criterion

Wenjing Shang [1], Yidong Xu [1], Junwei Qi [1,*], Wei Xue [1] and Sergey B. Makarov [2] ![ORCID]

[1] College of Information and Communication Engineering, Harbin Engineering University, Harbin 150001, China; shangwenjing@hrbeu.edu.cn (W.S.); xuyidong@hrbeu.edu.cn (Y.X.); xuewei@hrbeu.edu.cn (W.X.)

[2] Institute of Physics, Nanotechnology and Telecommunications, St. Petersburg State Polytechnical University, St. Petersburg 195251, Russia; makarov@cee.spbstu.ru

* Correspondence: qijunwei@hrbeu.edu.cn; Tel.: +86-139-4508-5246

Abstract: This paper presents a novel method designing an optimized waveform with high spectral efficiency based on minimum out-of-band radiation criterion. Introducing the Pan-function model, Fourier series, and constraints, we achieve the numeric solution of the optimized baseband signals. The optimal waveform provides an excellent bandwidth efficiency, and its bit error rate (BER) performance is improved using the minimum cross-correlation function. To verify the proposed model, we present a simulation of the signal modulation and demodulation schemes using MATLAB software. The results are consistent with expected results, verifying the correctness of this method.

Keywords: optimized waveform; spectral efficiency; Pan-function model

1. Introduction

Optimized signal waveform with features, higher utilization rate, lower peak-to-average power ratio (PAPR), and higher main lobe energy can be applied in many significant applications, such as mobile telecommunication, satellite communication, aircraft measurement, tracking, and controlling systems [1–3]. Previous studies have provided many effective optimization methods for different scenarios. In order to higher the utilization rate in band limited channel, modulations based on orthogonal frequency division multiplexing (OFDM) and quadrature amplitude modulation (QAM) are provided, both of which suffer from high PAPR [3–5]. Nonlinear characteristics of the transmitter amplifier lead to undesirable out-of-band radiation, which restrict the use of OFDM and QAM. Moreover, modulation with high PAPR is not suitable in nonlinear channel, where the signal spectrum could also be extended [1]. Efforts have been made in many studies to reduce the out-of-band radiation. In the work [6], minimum shift keying (MSK) is proposed, which is featured with constant envelope and has less out-of-band radiation compared with quadrature phase shift keying (QPSK). Furthermore, Gaussian filtered minimum shift keying (GMSK) shows better outband reduction compared with MSK, which takes the sacrifice of the constant envelope [7]. Pauli et al. [8] proposed the bandwidth efficient reduction of the crest factor (BERC) method.

In most canonical communication systems featured with constant or quasi-constant envelope, a rectangular base band signal is applied in QPSK, offset QPSK (OQPSK), and frequency-shift-keying (FSK)modulation systems; cosine signal is used in MSK and GMSK after filtering. These kinds of modulation systems show a lesser utilization rate compared with multiple carrier modulation. However, the contradiction between the utilization rate, main lode energy, and PAPR still needs further study. In recent years, there have been few studies giving mathematical optimization models based on certain criteria. In this paper, a novel method to design an optimized base band waveform is proposed based on minimum out-of-band radiation criterion and additional restrictions. In this method, we first give the target Pan-function based on the minimum out-of-band radiation criterion. Then,

we construct the boundary function with the restrictions, symbol boundary condition, single-symbol signal energy condition, constant-envelope condition, and minimum cross correlation function. Hence, Lagrange's equation is derived. After that, the base band waveform is discreted using Fourier series. The optimization problem is transmitted to finding the coefficient of the Fourier series, which could minimize the Lagrange's equation. To verify the proposed method, a communication system simulation model is set up. The numerical results show that the optimized waveform presents sharper roll-off, small out-of-band radiation, quasi-constant envelope, and good bit error rate (BER) performance.

2. Optimized Mathematical Modeling of the Optimized Waveform

2.1. Minimum Out-of-Band Radiation Criterion

In order to optimize the baseband symbol signals with higher spectral roll-off rate, an optimized mathematical function is established which minimizes the out-of-band radiation criterion [9] as

$$J = \frac{1}{2\pi} \int_{-\infty}^{+\infty} g(\omega)|S(\omega)|^2 d\omega \tag{1}$$

where $a(t)$ is the symbol signal waveform. It is an even function in the symbol period $[-T/2, T/2]$. $|S(\omega)|^2$ is the power spectrum of $a(t)$, and $g(\omega)$ is an increasing function that determines the roll-off rate of the spectral density function $S(\omega)$. The value of n determines the degree of suppressed out-of-band radiation. To achieve a convergent and integrable J, the roll-off rate of $|S(\omega)|^2$ should be greater than the rate of increase in $g(\omega)$ to limit the roll-off rate of the power spectrum $|S(\omega)|^2$ of the signal $a(t)$. Figure 1 plots the increasing function, $g(\omega) = \omega^{2n}(\omega > 0)$ versus n.
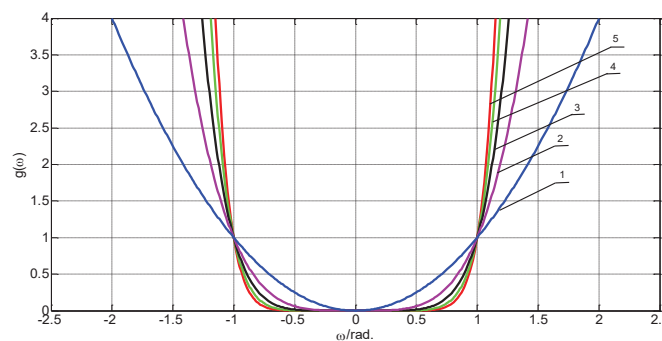

Figure 1. Waveforms of $g(\omega)$ for various n (i.e., from 1 to 5).

Following a series of mathematical manipulations (including Taylor series expansion [10]), Equation (1) may be written as

$$J = (-1)^n \int_{-T/2}^{T/2} a(t)a^{(2n)}(t)dt \tag{2}$$

where $a^{(2n)}(t)$ represents the $2n$-order derivative of the symbol signal. Equation (2) reveals that the criterion for minimum out-of-band radiation may be transformed into the problem of unraveling the symbol function $a(t)$ when minimizing the Pan-functional J.

2.2. Additional Constraints of the Pan-Function

As an example, we consider the partial-response quadrature modulation with a symbol length of $4T$. The analytic solution of the optimized mathematical model is fairly complex under restriction of the symbol boundary condition, single-symbol signal energy condition, constant-envelope condition,

and minimum cross-correlation function. However, we may obtain the optimized baseband signal waveforms using numerical calculation.

2.2.1. Restriction on the Symbol Boundary Condition

As is shown in [11], if $a(t)$, $a'(t)$, $a''(t)$, ... , $a^{(n-1)}(t)$ are continuous without skipping, and $a^{(n)}(t)$ is finite, then there is no skipping in the end point of the interval (i.e., the power spectrum of $a(t)$ could decay rapidly with the frequency). Herein, assuming that function $a(t)$ is within the interval $[-2T, 2T]$, it should satisfy the following boundary condition [1]:

$$a\left(\pm 2T\right) = a'\left(\pm 2T\right) = \ldots = a^{(n-1)}\left(\pm 2T\right) = 0 \tag{3}$$

2.2.2. Restriction on the Single-Symbol Signal Energy Condition

Considering the signal $a(t)$ with the length of $4T$, the energy per transmission can be expressed as

$$E = \int\limits_{-2T}^{2T} a^2\left(t\right)dt \tag{4}$$

2.2.3. Restriction on the Constant-Envelope Condition of the Quadrature-Modulated Signal

The constant-envelope modulation represents that the envelope of the modulated wave should be constant, the generated modulation signal is band-limited by the transmitter, and only a small spectrum spreading is produced after the signal passes through the nonlinear processing components [12]. Thus, the following conditions should be satisfied with t in the interval $[0, 4T]$

$$I^2(t) + Q^2(t) = const \tag{5}$$

Since the signal is symmetric, we only need to satisfy Equation (5) for t in the interval $[0, T]$. Then, the condition will be satisfied in the rest of the initial interval; i.e., $[T, 4T]$. In this case, the four symbols in the interval are defined as d_{-1}, d_0, d_1, d_2. The baseband signal of $I(t)$ and $Q(t)$ in the interval $[0, T]$ can be written as

$$I(t) = d_{-1}a(t + T) + d_1 a(t - T) \tag{6}$$

$$Q(t) = d_0 a(t) + d_2 a(t - 2T) \tag{7}$$

where d_{-1}, d_0, d_1, d_2 are the uncorrelated binary data symbols, each taking one of the values ± 1. The different conditions are as follows: For $d_{-1}d_1 = 1$, the adjacent baseband symbol signals take the same sign in the I channel.

If $d_0 d_2 = 1$, the adjacent baseband symbol signals take the same sign in the Q channel, and to meet the constant-envelope condition, we should introduce the attenuation factor r in $[0, 1]$, yielding

$$\begin{aligned} I_{11}^2(t) &= r^2 a^2(t - T) + 2ra(t + T)a(t - T) + a^2(t + T) \\ Q_{21}^2(t) &= r^2 a^2(t) + a^2(t - 2T) + 2ra(t)a(t - 2T) \end{aligned} \tag{8}$$

If $d_0 d_2 = -1$, the adjacent baseband symbol signals take opposite signs in the Q channel, we have

$$\begin{aligned} I_{12}^2(t) &= a^2(t - T) + 2a(t + T)a(t - T) + a^2(t + T) \\ Q_{22}^2(t) &= r^2 a^2(t) + a^2(t - 2T) - 2ra(t)a(t - 2T) \end{aligned} \tag{9}$$

The constant value of the envelope is set to be $a(0)$, which is the value of $a(t)$ at time $t = 0$, and is also the maximum value of the signal $a(t)$. To ensure that the modulated signal always has a constant envelope in the interval $[0, T]$, the constant-envelope condition is rewritten as

$$\int_0^T \left(I_{11}^2(t) + Q_{21}^2(t) - a^2(0) \right)^2 dt = 0 \tag{10}$$

$$\int_0^T \left(I_{12}^2(t) + Q_{22}^2(t) - a^2(0) \right)^2 dt = 0 \tag{11}$$

Similarly, if $d_{-1}d_1 = 1$, the adjacent baseband symbol signals take the opposite signs in the I channel. The constant envelope conditions may be obtained as

$$\int_0^T \left(I_{13}^2(t) + Q_{23}^2(t) - a^2(0) \right)^2 dt = 0 \tag{12}$$

$$\int_0^T \left(I_{14}^2(t) + Q_{24}^2(t) - a^2(0) \right)^2 dt = 0 \tag{13}$$

Thus, the constant-envelope conditions in the interval $[0, T]$ can be expressed as follows:

$$\int_0^T \left\{ \begin{array}{l} \left[I_{11}^2(t) + Q_{21}^2(t) - a^2(0) \right]^2 + \left[I_{12}^2(t) + Q_{22}^2(t) - a^2(0) \right]^2 \\ + \left[I_{13}^2(t) + Q_{23}^2(t) - a^2(0) \right]^2 + \left[I_{14}^2(t) + Q_{24}^2(t) - a^2(0) \right]^2 \end{array} \right\} dt = 0 \tag{14}$$

2.2.4. Restriction on the Minimum Cross-Correlation Function

The intersymbol interference (ISI) lowers the correlation performance in a partial-response system, increasing the bit error rate (BER). In order to improve the receiving reliability, additional restrictions are introduced, including single-symbol energy, boundary condition, constant-envelope, and minimum cross-correlation function. Three random baseband symbols and eight types of waveforms exist in the interval $[-2T, 2T]$, in orthogonal or in-phase channel. Eight different waveforms yield 36 combinations in Euclidean distances. We may express the minimum Euclidean distance between each two waveforms as

$$d_{\min}^2 = \min\left\{ d_{\{a_i,a_j\}}^2 \right\} = \min_{i,j} \int_{-2T}^{2T} \left(a_i(t) - a_j(t) \right)^2 dt = \min\left\{ d_{i,j}^2 \right\} \tag{15}$$

where $a_i(t)$ is the waveform in the interval $[-2T, 2T]$, $i = 1, 2, \ldots, 8$. Figure 2 shows all possible composed modes of three random baseband symbols in the interval $[-2T, 2T]$. In contrast, Figure 3 plots the synthetic waveform of three random baseband symbols in the interval $[-2T, 2T]$. Table 1 lists the Euclidean distance between two waveforms.
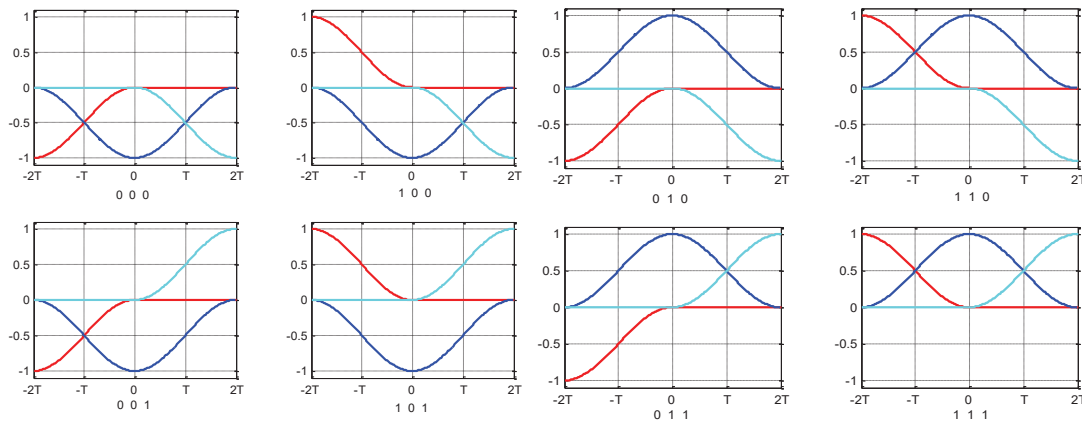
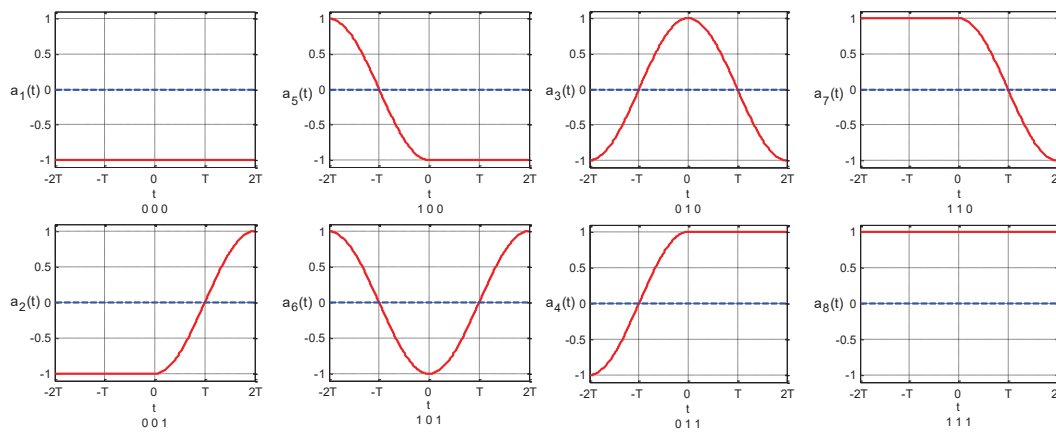**Figure 2.** Composed modes of three random baseband symbols in the interval $[-2T, 2T]$.

Figure 3. Synthetic waveforms of three bits random baseband symbols in the interval $[-2T, 2T]$.

Table 1. Euclidean distance between any two waveforms.

d_{ij}	$j=1$	$j=2$	$j=3$	$j=4$	$j=5$	$j=6$	$j=7$	$j=8$
$i=1$	0	$2E$	$4E$	$6E+8K$	$2E$	$4E$	$6E+8K$	$8E+8K$
$i=2$	-	0	$6E-8K$	$4E$	$4E$	$2E$	$8E$	$6E+8K$
$i=3$	-	-	0	$2E$	$6E-8K$	$8E-16K$	$2E$	$4E$
$i=4$	-	-	-	0	$8E$	$6E-8K$	$4E$	$2E$
$i=5$	-	-	-	-	0	$2E$	$4E$	$6E+8K$
$i=6$	-	-	-	-	-	0	$6E-8K$	$4E$
$i=7$	-	-	-	-	-	-	0	$2E$
$i=8$	-	-	-	-	-	-	-	0

$$
\begin{aligned}
d^2{}_{i,j} &= \int_{-2T}^{2T} (a_i(t) - a_j(t))^2 dt \\[2mm]
K &= \int_{-2T}^{2T} a(t) \cdot a(t - 2T) dt \\[2mm]
E &= \int_{-2T}^{2T} a^2(t) dt
\end{aligned}
\tag{16}
$$

We obviously see that decreasing K leads to increasing the minimum Euclidean distance, for a constant symbol energy E. Therefore, the minimum cross-correlation function K may restrict the improvement of the BER performance. The autocorrelation function in $[0, 2T]$ can be defined as

$$K = \int_0^{2T} a(t) \cdot a(t - 2T) \, dt \tag{17}$$

we have

$$\int_0^{2T} (a(t) \cdot a(t - 2T) - K/2T) \, dt = 0 \tag{18}$$

Introducing the Fourier series and additional restrictions, single-symbol energy, constant envelope condition after modulation and minimum cross-correlation function, the Pan-function can be expressed as

$$
\begin{aligned}
H &= J + \lambda \left(\int_{-2T}^{2T} a^2(t) dt - E \right) + \mu \int_0^{2T} [a(t) \cdot a(t - 2T) - K/2T] dt \\
&\quad + \gamma \int_0^T \{ [I_{11}^2(t) + Q_{21}^2(t) - a^2(0)]^2 + [I_{12}^2(t) + Q_{22}^2(t) - a^2(0)]^2 \\
&\quad + [I_{13}^2(t) + Q_{23}^2(t) - a^2(0)]^2 + [I_{14}^2(t) + Q_{24}^2(t) - a^2(0)]^2 \} dt
\end{aligned}
\tag{19}
$$

where λ, μ, and γ are Lagrange constants. H is the Lagrange function.

2.3. Signal Solving Process Using Fourier Series

A periodic function in the interval $[-2T, 2T]$ may be expressed by Fourier series expansion [13]. Therefore, the efficient spectrum signal $a(t)$—as an even function with the width of $4T$—can be written as

$$a(t) = \frac{a_0}{2} + \sum_{k=1}^{m} \left(a_k \cos(\frac{\pi}{2T} kt) \right) \tag{20}$$

where

$$a_0 = (1/2T) \int_{2T}^{2T} a(t) dt$$

$$a_k = (1/2T) \int_{-2T}^{2T} a(t) \cos(\pi kt/2T) dt$$

Then, substituting Equation (20) into Equation (19), yielding

$$
\begin{aligned}
H &= 2T \sum_{k=1}^{m} a_k^2 (\frac{\pi}{2T} k)^{2n} + \lambda \{ \frac{E}{2T} - [2 \sum_{k=1}^{m} (-1)^{k+1} a_k]^2 - \sum_{k=1}^{m} a_k^2 \} \\
&\quad + \mu \int_0^{2T} [a(t) \cdot a(t - 2T) - K/2T] dt + \gamma \int_0^T ((I_{11}^2(t) + Q_{21}^2(t) - a^2(0))^2 \\
&\quad + (I_{12}^2(t) + Q_{22}^2(t) - a^2(0))^2 + (I_{13}^2(t) + Q_{23}^2(t) - a^2(0))^2 \\
&\quad + (I_{14}^2(t) + Q_{24}^2(t) - a^2(0))^2) dt
\end{aligned}
\tag{21}
$$

Based on the extreme value theory of the variational calculus [14], Equation (21) should satisfy the following partial differential equations

$$\begin{aligned} \frac{\partial H}{\partial a_k} &= 0; k = 1, 2, \ldots, m \\ \frac{\partial H}{\partial \lambda} &= 0, \frac{\partial H}{\partial \mu} = 0, \frac{\partial H}{\partial \gamma} = 0 \end{aligned} \tag{22}$$

The normalizations are defined as $E = 1$ and $T = 1$. Thus, the coefficients, $a_0, a_1, \ldots, a_m$ of the Fourier series, and the Lagrange constants, λ and μ, are the unknown parameters. The solution of simultaneous equations is used to determine the values of the unknown coefficients, $a_0, a_1, \ldots, a_m$ of the Fourier series. We introduce envelope fluctuation coefficient to determine the constant envelope properties. The envelope fluctuation coefficient is defined as

$$\varepsilon = \frac{e_{\max} - e_{\text{ave}}}{e_{\text{ave}}} \tag{23}$$

where $e_{\max}$ represents the maximum value of the envelope and e_{ave} denotes the average value of the envelope. Table 2 shows the coefficient of the Fourier series for different m and n. Figure 4 shows the corresponding time domain curves.

Table 2. The unknown coefficient of the Fourier series in Equation (20).

n	m	a_0	a_1	a_2	a_3	a_4	a_5	a_6	a_7
1	4	0.660	0.5000	0.1793	−0.001865	−0.01111	-	-	-
3	5	0.6364	0.4998	0.2152	0.01092	−0.03402	−0.01126	-	-
5	6	0.6280	0.4992	0.2266	0.02026	−0.03790	−0.02006	−0.003333	-
7	7	0.6310	0.4995	0.2224	0.01635	−0.03726	−0.01671	−0.001131	0.0004888
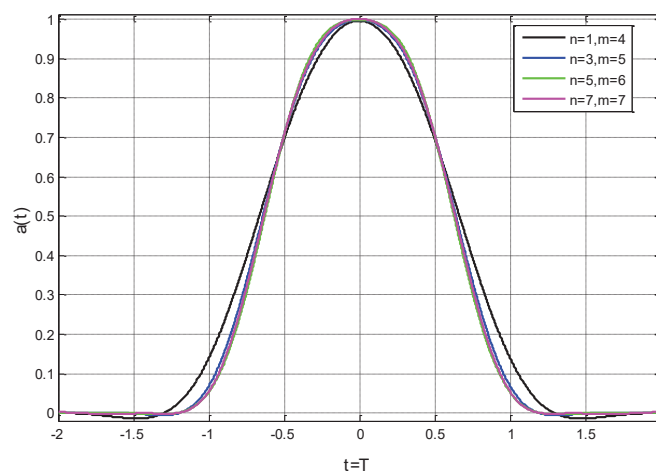
Figure 4. Waveform of the optimized baseband signals.

Figure 5 shows the normalized power spectra curves of optimized signal, where curve 1 corresponds to the MSK and curves 2–5 correspond to $[n = 1, m = 4]$, $[n = 3, m = 5]$, $[n = 5, m = 6]$, and $[n = 7, m = 7]$, respectively.
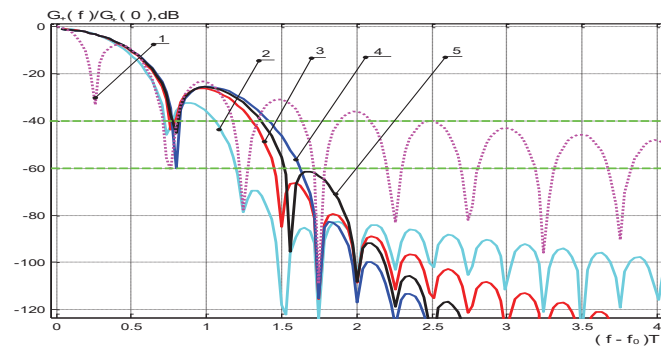
Figure 5. Normalized power spectra curves of the optimized signals. Curve 1 corresponds to the MSK and curves 2–5 correspond to $[n = 1, m = 4]$, $[n = 3, m = 5]$, $[n = 5, m = 6]$, and $[n = 7, m = 7]$, respectively.

Table 3 considers different pairs of n and m, and presents the bandwidth, where the normalized power spectra of the optimized signals decreased as -40 dB (ΔF_{-40dB}) and -60 dB (ΔF_{-60dB}). Table 3 also lists the value of the bandwidth, where 90% and 99% of the signal energy is achieved (i.e., $\Delta F_{90\%}$ and $\Delta F_{99\%}$, respectively). Besides, the corresponding envelope fluctuation coefficient ε and the cross-correlation function K of the optimized signal are presented in the last two columns of Table 3.

Table 3. Comparison of the characteristics of the signals of the energy spectrum and K. MSK: minimum shift keying.

Waveform	ΔF_{-40dB}	ΔF_{-60dB}	$\Delta F_{90\%}$	$\Delta F_{99\%}$	$\varepsilon\,(10^{-2})$	$K\,(10^{-5})$
$n=1, m=4$	1.09	1.21	0.72	1.06	6.70	6.84
$n=3, m=5$	1.30	1.44	0.78	1.17	0.74	-7.52
$n=5, m=6$	1.43	1.61	0.79	1.20	0.45	-2.64
$n=7, m=7$	1.35	1.50	0.80	1.22	0.52	-11.52
MSK	2.5	8.0	0.78	1.2	0.0	0.0

Figure 5 and Table 3 reveal that for the minimum out-of-band energy radiation criterion with the restrictions, the optimized efficient spectrum signal presents the bandwidth of $1.09/T$ (for $n = 1$ and $m = 4$, calculated according to -40 dB) and $1.21/T$ (for $n = 1$ and $m = 4$, calculated according to -60 dB). Moreover, the bandwidths of ΔF_{-40dB} and ΔF_{-60dB} have been decreased to 43.6% and 15.13% of that of the MSK signal, respectively. This verifies that the signal's out-of-band radiation is prevented. Applying the optimized efficient spectrum signal as the baseband modulation signal, the modulated signal after the quadrature modulation presents the envelope characteristics. Moreover, the cross-correlation function K of the optimized baseband signal is too small, which reduces the inter-symbol interference and increases the reliability of the receiving.

3. Simulation and Realization of the System

3.1. Scheme of the Modulation and Demodulation Systems

Figure 6 illustrates the block diagram of the adopted partial-respond quadrature modulation scheme. Three serial-to-parallel (S/P) converters convert the group of symbols d_i, $i = 0, 1, \ldots, \infty$, with a symbol duration of T into four blocks, each taking one of the values ± 1, where the delay time is a different integer multiple of T while the symbol duration has increased to $4T$. The symbols enter cross-correlator, and according to the results of the cross-correlation operation, the symbol attenuation factor r was introduced. Then, the output signals of the pulse shaping filter provides the signals $I(t)$

and $Q(t)$ in two channels. The signals $I(t)$ and $Q(t)$ were multiplied to the quadrature carrier and added to achieve the modulated signal.
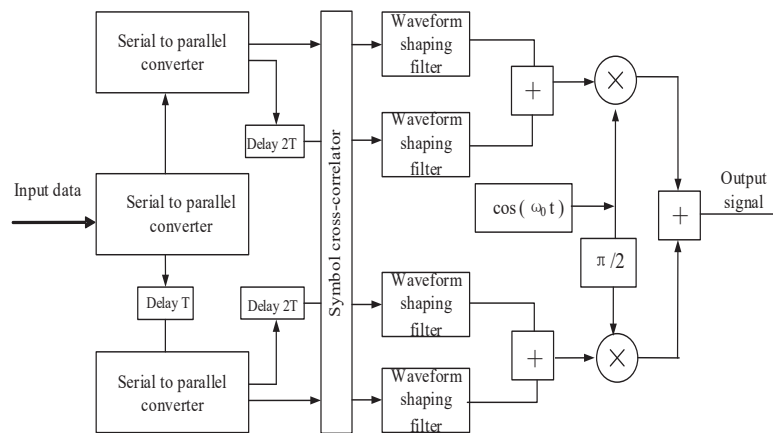

Figure 6. Block diagram of the quadrature modulation system.

Figure 7 depicts the block diagram representation of the coherent demodulation of the signals. To remove the high-frequency components of the received modulated signal, it is coherently demodulated through the quadrature carriers and the low-pass filters. Since the signal in each channel introduces intersymbol interference, the baseband signal is filtered by a match filter. The signal on each channel is integrated, where the integration time is controlled by the integrator strobe pulse. Finally, the demodulation process follows the sampling, decision, and a P/S converter.
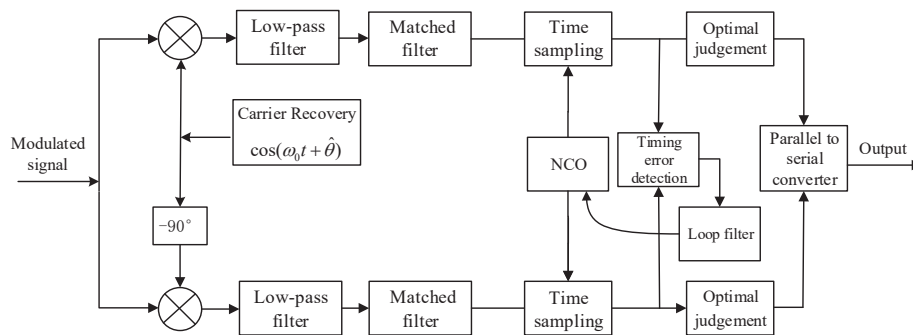

Figure 7. Block diagram of the partial-respond coherent demodulation. NCO: numerical control oscillator.
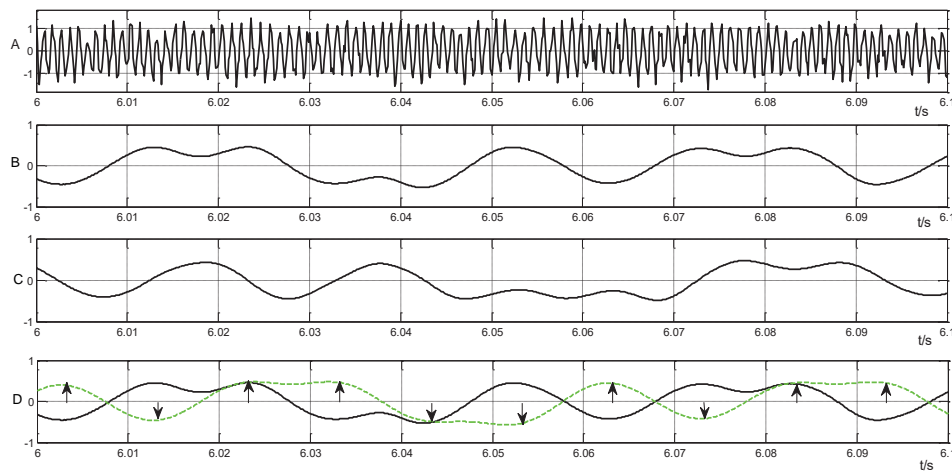
3.2. Simulation Results

We simulated the quadrature modulation and coherent demodulation using the MATLAB software, where an optimized signal was used for the baseband symbol. Figure 8 presents the simulation results, where A represents the baseband symbol signal transmitted through the in-phase channel, B is the baseband symbol signal transmitted via the orthogonal channel, and C is the quadrature-modulated output signal. The envelope of the output signal after the modulation was found to be constant, and in agreement with the expected results.
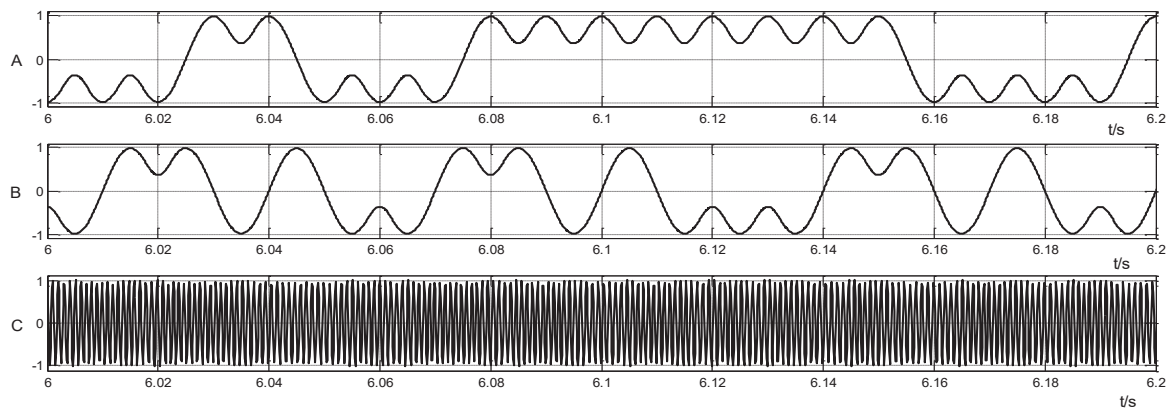
Figure 8. Simulation results of the partial-respond quadrature modulation. (**A**): The baseband symbol signal transmitted through the in-phase channel; (**B**): The baseband symbol signal transmitted via the orthogonal channel; (**C**): The quadrature-modulated output signal.

Figure 9 plots the simulation results of the coherent demodulation, where A indicates the transmitted signal corrupted with additive white Gaussian noise (AWGN), which is the input of the receiver, B is the baseband signal demodulated in the in-phase channel, and C is the baseband signal demodulated in the orthogonal channel. The black solid and green dotted lines in D represent the baseband signal demodulated in the in-phase channel and the baseband signal through the matched filter, respectively, while the arrows show the best sampling time [1,15,16].

Figure 9. Simulation results of partial-respond demodulation system. (**A**): The transmitted signal corrupted with additive white Gaussian noise; (**B**): The baseband signal demodulated in the in-phase channel; (**C**): The baseband signal demodulated in the orthogonal channel; (**D**): The baseband signal through the matched filter and best sampling time.

Figure 10 compares the BER performance of the optimized baseband signals achieved with and without minimum cross-correlation function [17]. We may notice from this figure that for small E_b/N_0s, the BER performances of the optimized baseband with and without minimum cross-correlation function restriction are close. However, when $BER = 10^{-3}$, the E_b/N_0s of the optimized baseband signal with and without minimum cross-correlation function restriction are 6.8 dB and 7.0 dB, reducing 0.2 dB in the requirement of E_b/N_0. For, $BER = 10^{-4}$, the E_b/N_0s of the optimized baseband signal with and without minimum cross-correlation function restriction are 8.3 dB and 8.6 dB, respectively, which reduces 0.3 dB in the requirement of E_b/N_0. The results show that the optimized baseband

signals with minimum cross-correlation function have superior spectral efficiency and the BER performance can be improved by introducing the minimum cross-correlation function restriction.
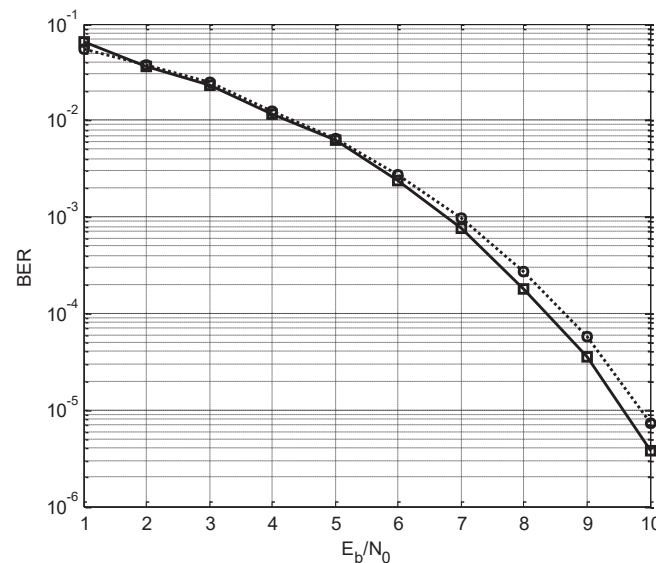

Figure 10. Bit error rate (BER) curves of the simulation system.

4. Conclusions

A Pan-functional model was established to present optimized efficient spectrum signals based on the minimum out-band energy radiation criterion. The achieved signals provide higher out-band spectral roll-off rate with quasi-constant envelope. This is due to the introduction of the controlled ISI, which are greatly superior to that of the QPSK and MSK signals in frequency spectral. Limiting the minimum Euclidean distance, ISI may slightly affect the adjacent baseband symbol signal reception, and improve the performance of the system. We presented the simulation results of the signal modulation and demodulation schemes with controlled ISI, which have been carried out using the MATLAB software. The results reveal that by taking the restriction of the minimum cross-correlation function into account, for the BER of 10^{-4}, the E_b/N_0 reduces by 0.3 dB. As a future work, we will investigate how to optimize the multi-frequency signals (e.g., OFDM systems) to further improve the achievable spectral efficiency.

Author Contributions: Wenjing Shang did the mathematical modeling and the simulations. She also wrote the draft of the paper. Yidong Xu contributed to the revisions and the discussion of the results. Junwei Qi, Wei Xue and Sergey B. Makarov put forward the idea and checked the simulation of this paper.

Conflicts of Interest: The authors declare no conflict of interest.

References

1. Simon, M.K. *Bandwidth-Efficient Digital Modulation with Application to Deep-Space Communications*; John Wiley & Sons: Hoboken, NJ, USA, 2003; Volume 2.
2. Han, S.H.; Lee, J.H. An overview of peak-to-average power ratio reduction techniques for multicarrier transmission. *IEEE Wirel. Commun.* **2005**, *12*, 56–65.
3. Boonkajay, A.; Adachi, F. A blind selected mapping technique for low-PAPR single-carrier signal transmission. In Proceedings of the International Conference on Information, Communications and Signal Processing, Singapore, 2–4 December 2015; pp. 1–5.

4. Falconer, D. Linear Precoding of OFDMA Signals to Minimize Their Instantaneous Power Variance. In Proceedings of the Wireless Communications and NETWORKING Conference, Sydney, Australia, 18–21 April 2010; pp. 1–6.

5. Kawamura, T.; Kishiyama, Y.; Higuchi, K.; Sawahashi, M. Comparisons of 16QAM Modulation Schemes Considering PAPR for Single-Carrier FDMA Radio Access in Evolved UTRA Uplink. In Proceedings of the IEEE Ninth International Symposium on Spread Spectrum Techniques and Applications, Manaus-Amazon, Brazil, 28–31 August 2006; pp. 332–336.

6. Pasupathy, S. Minimum shift keying: A spectrally efficient modulation. *IEEE Commun. Mag.* **1979**, *17*, 14–22.

7. Goode, S.H. A comparison of Gaussian minimum shift keying to frequency shift keying for land mobile radio. In Proceedings of the 34th IEEE Vehicular Technology Conference, Pittsburgh, PA, USA, 21–23 May 1984; Volume 34, pp. 136–141.

8. Pauli, M.; Kuchenbecker, P. On the reduction of the out-of-band radiation of OFDM-signals. In Proceedings of the IEEE International Conference on Communications (ICC98), Atlanta, GA, USA, 7–11 June 1998; Volume 3, pp. 1304–1308.

9. SHKOL'NYY, L.A. The Minimum Out-of-Band Radiation Optimization of Radio Pulse Shape. *Radio Technol.* **1975**, *30*, 12–15.

10. Xue, W.; Ma, W.; Chen, B. A realization method of the optimized efficient spectrum signals using fourier series. In Proceedings of the 2010 6th International Conference on Wireless Communications, Networking and Mobile Computing (WiCOM), Chengdu, China, 23–25 September 2010.

11. Mason, S.J.; Zimmermann, H.J. *Electronic Circuits, Signals and Systems*; Wiley: New York, NY, USA, 1960.

12. Liu, L.; Liang, J. Clipping based MC-CDMA system with lower peak-to-average power ratio. *Comput. Eng. Appl.* **2007**, *43*, 129–132.

13. Haykin, S.; Van Veen, B. *Signals and Systems*; Wiley: New York, NY, USA, 2002.

14. Hu, H.; Hu, R. *Calculus of Variations*; China Architecture and Building Press: Beijing, China, 1987.

15. He, X.; Pei, C.; Meng, Y. A baseband GMSK signal correlator and its output probability distribution. *J. Electron. Inf. Technol.* **2009**, *32*, 2532–2535.

16. Zhao, H.; Zhao, D.; Hou, C. Design and Implementation of MSK Modem. *J. Harbin Univ. Sci. Technol.* **2011**, *16*, 102–106.

17. Xu, Y.; Xue, W.; Shang, W. A Pan-Function Model for the Utilization of Bandwidth Improvement and PAPR Reduction. *Math. Probl. Eng.* **2014**, *2014*, doi:10.1155/2014/658093.